

I. KALEMBA-REC^{1*}, M. KOPYŚCIAŃSKI¹, P. ŚLIWIŃSKI², S. DYMEK¹,
M.S. WĘGŁOWSKI², A. WRONA³, K. GROŃ

IMPACT OF LASER REMELTING PARAMETERS ON THE MICROSTRUCTURE AND PROPERTIES OF SPRAYED Ni20Cr COATINGS WITH RHENIUM ADDITION

The study was focused on the characterization of microstructural evolution and microhardness in the plasma-sprayed and laser remelted Ni-Cr coatings with 20% addition of rhenium on stainless steel. The remelting process was performed with different laser power and laser traverse speed. The laser remelting process improves the quality of plasma sprayed Ni-Cr-Re coatings, reducing the porosity and the inhomogeneity of the chemical composition. The remelted coatings were characterized by a dendritic microstructure. Microsegregation of rhenium to dendrites was observed. The remelted coatings have an iron content of over 40%, which is the result of too deep remelting with the substrate material. The iron content in the remelted coatings increases with the decrease in laser speed, but the rhenium content decreases. All tested coatings were characterized by hardness similar to that of the substrate material.

Keywords: Ni-Cr-Re Coatings; Laser Remelting; Plasma Spraying; Microstructure

1. Introduction

In numerous applications, mechanical components must endure harsh conditions, including high loads, speeds, temperatures, and corrosive environments. Therefore, surface modification becomes essential to protect them from various forms of deterioration. Coatings, fabricated through thermal spray techniques, find extensive application across various industries, providing wear and erosion resistance, corrosion protection, and thermal insulation [1-3].

The plasma-spray coating technique is extensively used in surface engineering to streamline processing and reduce operational and maintenance costs across various industries. Its usage spans transportation sectors (including shipbuilding, automotive, and aerospace), mechanical manufacturing, tooling, chemical processing, biomedical fields, and beyond. Coatings play a crucial role in engineering by safeguarding against wear, friction, corrosion, and providing thermal protection in high-temperature environments. Given that most products encounter harsh, corrosive, and high-temperature conditions during service life, ensuring protection against deterioration is paramount to enhancing the reliability and performance of engineering

components. Addressing any flaws in plasma-sprayed coatings is crucial to realizing their intended purposes. Inherent defects such as pores (porosity), un-melted or partially melted particles, and cracks can adversely affect the mechanical, physical, and chemical properties of these coatings. Porosity, a typical feature of plasma-sprayed coatings, can especially compromise their protective performance within demanding working environments [3-6].

However, it should be noted that during high-energy processes (such as laser beam or electron beam), solidification occurs under non-equilibrium conditions. Remelting the produced coatings makes it possible to reduce coating porosity and improve its adhesion, especially when the entire coating thickness, up to the substrate material, undergoes melting. Previous research has shown that in most cases, reducing porosity and simultaneously increasing hardness is achievable only by remelting the coating using a laser or electron beam. The very high-power densities associated with laser and electron beams induce rapid heating, melting, and fast cooling of the coating material. By adjusting the power density and linear energy, it is possible to precisely control the depth of the remelted material and thus the properties of final coatings. The remelting process of surface layers also

¹ AGH UNIVERSITY OF KRAKOW, FACULTY OF METALS ENGINEERING AND INDUSTRIAL COMPUTER SCIENCE, AL. MICKIEWICZA 30, 30-059 KRAKOW, POLAND

² LUKASIEWICZ – UPPER SILESIAN INSTITUTE OF TECHNOLOGY, 44-100 GLIWICE, POLAND

³ LUKASIEWICZ – INSTITUTE OF NON-FERROUS METALS, 44-121 GLIWICE, POLAND

* Corresponding Author: kalemba@agh.edu.pl



allows for the reduction of surface roughness and the decrease of residual stresses [7-11].

The main objective of this research is to investigate and analyze the phenomena occurring during the laser remelting of plasma-sprayed coatings made of Ni-Cr-Re alloys on stainless steel. The addition of Re aims to increase wear and heat resistance compared to typical Ni-Cr alloys. Rhenium, a rare element with an atomic number of 75, an atomic mass of 186.2, and a very high melting point of 3186°C, is characterized by high hardness, density, corrosion resistance, and resistance to deformation. These properties make it suitable for use in alloys and coatings with high creep resistance at high temperatures. Majchrowicz et al. [12] observed that the inclusion of rhenium in SLM-processed IN718-Re alloys resulted in the segregation and accumulation of rhenium in the γ phase dendrites. As the amount of rhenium increased, the columnar/cellular substructures became wider. The addition of rhenium to the IN718 alloy enhanced its corrosion resistance in Na₂SO₄ and NaCl solutions on both exposed surfaces. Furthermore, Sanghoon Noh et al. [13] conducted a study to examine the influence of rhenium inclusion on the microstructures and mechanical properties of 15Cr-1Mo ferritic steels. The study entailed the production of components with incorporated rhenium through the utilization of mechanical alloying, hot isostatic pressing, and hot rolling techniques. The microstructure analysis revealed minimal deviations in grain morphologies and nano-oxide distributions. The addition of 0.5 wt.% rhenium to these ferritic steels led to higher tensile and creep strengths at elevated temperatures compared to steels without rhenium. Therefore, it can be deduced that incorporating rhenium into nickel or iron alloys has the capacity to improve their mechanical and corrosion resistance properties. Above mentioned papers are great literature examples of rhenium influence on steels and nickel alloys. Kurzynowski T. et al. [14], employed laser surface alloying (LSA) with rhenium to produce wear and corrosion-resistant layers on the Inconel 718 alloy. Two alloyed layers were produced using a high-power diode laser and a laser track overlapping ratio of 50%. The first layer consisted of IN718 alloy with 14 wt.% Re, where the Re powder was completely dissolved in the substrate. The second layer consisted of IN718 alloy with 28 wt.% Re, where the Re powder was partially dissolved in the substrate. The microstructure and tribological characteristics of both the substrate and the alloyed layers were analyzed under sliding and abrasive wear conditions. Additionally, electrochemical measurements were conducted in a 3 wt.% NaCl solution. The addition of 14 wt.% Re to IN718 was found to enhance its corrosion resistance. This is supported by the observed shift in the corrosion potential (+100 mV) and a significant increase in the critical pitting potential (+270 mV), while experiencing a 24% reduction in corrosive current. The layer that was alloyed with 28 wt.% Re exhibited a significant enhancement in hardness, with a 160% increase compared to the IN718 substrate. Additionally, it demonstrated a substantial reduction in sliding wear rate, with an 82% decrease, and a notable improvement in abrasive wear resistance, with a 25% increase in the resistance index.

However, producing high-quality wear resistance coatings constitutes a great challenge from both a scientific and practical point of view. In this study, the laser remelting process was used to eliminate pores, enhance the adhesion, homogenise of chemical composition and improve mechanical properties of the plasma sprayed coatings. Hence, the aim of this study was to determine the influence of laser remelting parameters (laser power and laser traverse speed) on the microstructure and microhardness of Ni-Cr-Re coatings.

2. Materials and experimental procedures

2.1. Materials

The subject of the research was plasma-sprayed and laser-melted Ni-Cr coatings with 20% addition of rhenium on 316Ti steel. 316Ti steel (designated according to PN-EN 1.4571 with a chemical composition of X6CrNiMoTi17-12-2) is an austenitic chromium-nickel-molybdenum steel characterized by resistance to intergranular corrosion, pitting corrosion, and resistance to the presence of acids and salts, including sulfuric acid, organic acids, nitrates, bromides and chlorides.

The plasma spraying process was conducted by an atmospheric AP-50 plasma spraying system (Flame Spray Technologies) at the Lukaszewicz Research Network – Institute of Non-Ferrous Metals. In the plasma spraying process a nickel-chromium (Ni20Cr) powder with a 20 wt.% addition of rhenium was applied. The methodology of powder preparation and the characterization of applied powders were presented in [15]. The plasma spraying parameters are collected in TABLE 1.

TABLE 1

Plasma spraying parameters

Voltage		69 V
Arc current		530 A
Plasma gas	Plasma gas flow rate (Ar)	54 l/min
	Plasma gas flow rate (H ₂)	9 l/min
Powder carrier gas	Transport gas flow rate (Ar)	5 l/min
Spraying distance (torch- surface)		0.14 m
Speed of movement		0.4 m/s

The plasma sprayed coatings were remelted by laser beam. The laser melting process was carried out on a robotic workstation equipped with a Yb:YAG solid-state laser Trumpf Trudisk 12002 at the Lukaszewicz Research Network – Welding Institute. The applied remelting parameters were narrowed down based on previous experiences with CO₂ laser remelting of Ni-Cr-Re layers. Only paths which visual condition was acceptable (no visible macroscale cracks, pores and other inconsistencies) were used for further testing. The laser traverse speed was varied in the range of 0.3-0.5 m/s, while the laser power ranged from 1900 to 2500 W. Three passes were applied on each field. The overlap between the paths was about 30% of their width. For the D70 head, the beam transmission system was configured with an

optical fibre with a core diameter of 0.0003 mm and a collimator lens with a focal length of 0.2 m and a focusing lens with a focal length of 0.2 m. The working head was then raised by 0.03 m, leading to defocusing the beam on the surface of the material to increase its diameter. Thus, the diameter of the laser beam on the surface of the coating was 0.0048 m. Between melting of each subsequent field, the plate was cooled in atmosphere to room temperature. The research examined four samples after the laser melting process with different laser powers and traverse speeds (TABLE 2). For comparison purposes, the amount of heat transferred into the coating has been presented as linear energy (J/mm) without taking into account the thermal efficiency coefficient due to the nature of the laser as a heat source, for which the actual value of this coefficient strongly depends on the type of surface being remelted and the power of the laser beam. All remelted coatings were made of the same material thus for this reason the thermal efficiency coefficient was omitted. The linear energy was determined from the formula:

$$Q = P / (v * 1000 / 60)$$

Q – linear energy, J/mm; P – laser power, W; v – laser traverse speed, m/min.

Another very important value is the resulting power density of the laser on the remelted surface. The power density on the remelted surface was determined from the formula:

$$S = \frac{P}{\pi \left(\frac{d}{2}\right)^2}$$

S – power density, W/mm²; P – laser power; d – laser beam diameter on the remelted surface.

TABLE 2

The parameters of the laser melting process

Sample number	Laser beam power [W]	Laser traverse speed [m/min]	Linear energy [J/mm]	Power density on the surface [W/mm ²]
1	1900	0.5	228	105
2	2100	0.5	252	116
3	2500	0.5	300	138
4	1900	0.3	380	105

2.2. Methodology

The research consisted of microstructural analysis of plasma sprayed and laser remelted coatings and microhardness testing. The microstructural observations were performed on cross-sections of the coatings using a Zeiss Axio Imager M1m light microscope (LM) and a FEI Inspect S50 scanning electron microscope (SEM). For microscopic examinations the samples were polished and electrolytically etched in a 10% solution of chromium (VI) oxide in water. The SEM investigations were performed at an accelerating voltage of 5-15 kV. Additionally, EDS analysis (by EDAX Octan Elect detector) was carried out.

The chemical composition of coatings and microsegregation of elements (in the dendrites and interdendritic spaces) were analysed. The roughness of plasma sprayed coatings was examined by Wyko NT9300 optical profilometer. Microhardness measurements were conducted using a Wilson TUKON 2500 microhardness tester. Microhardness was determined on the Vickers scale (HV), using a load force of 3 N for 10 s. Microhardness of the sprayed coating was measured in 10 random locations. For the remelted coatings hardness measurement points were spaced at 0.1 mm intervals, starting from the substrate material, through the heat-affected zone and the remelted coating, to the sample surface. Measurements were performed in two melt zones – at the first and the deepest passes.

3. Results and discussion

The microstructure of the plasma sprayed coating is shown in Fig. 1. The plasma-sprayed coating was characterized by significant roughness ($R_a = 20.4 \pm 1.5 \mu\text{m}$), high porosity and chemical heterogeneity. The average thickness of the Ni-Cr-Re coating was equal to $255.8 \pm 21.8 \mu\text{m}$. The thickness of the Ni-Cr-Re coating was equal to approx. 250 μm . Fig. 1c presents the EDS results for the selected area of plasma-sprayed coatings. The results show some differences in distribution of elements: nickel-chromium areas, rhenium areas and mixed areas of Ni, Cr and Re were revealed in the coatings.

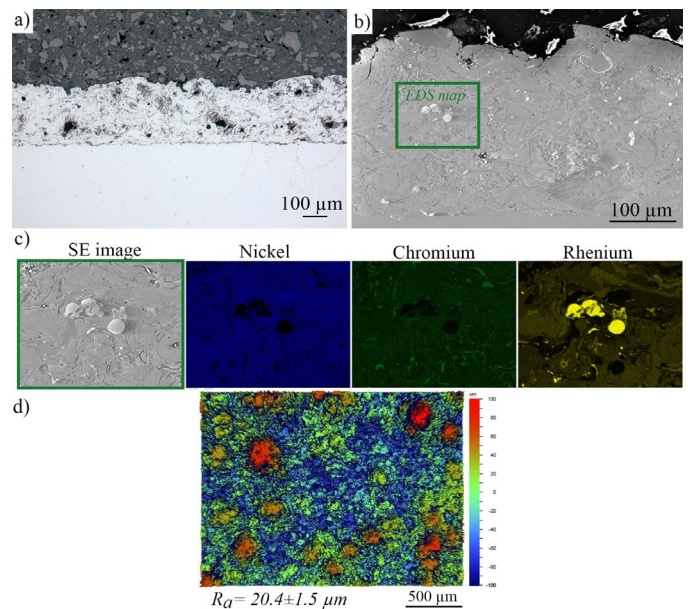


Fig. 1. Microstructure of cross-section of plasma sprayed Ni-Cr-Re coating a) LM image, b) SEM image, c) EDS mapping of the marked area, d) roughness map

In Fig. 2 the macrostructure of remelted coatings (with remelts widths indicated) is presented. After the remelting process, the following zones were observed in the analysed samples: the remelted zone (coating), the fusion line and the base material. The coatings consisted of overlapping paths of the

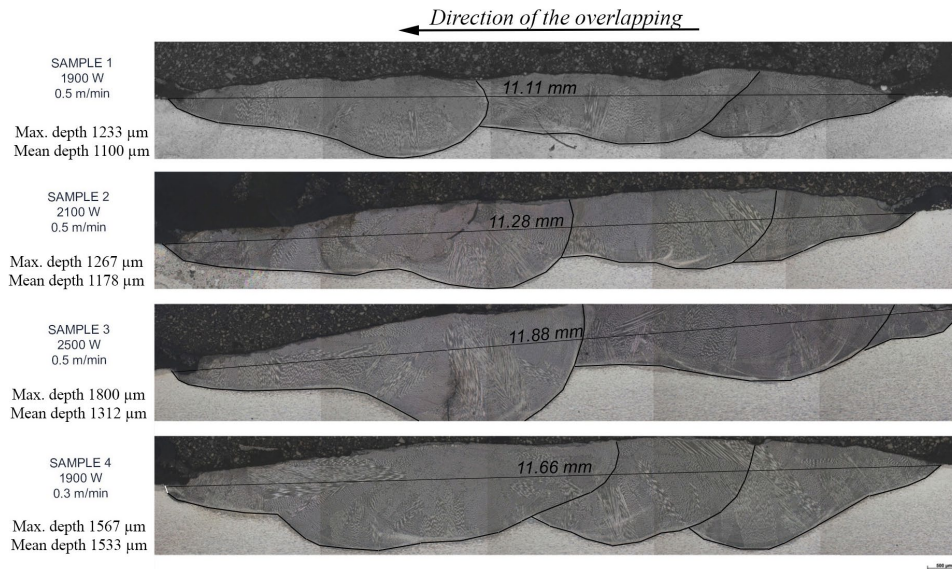


Fig. 2. Macrostructure of plasma sprayed coatings after laser remelting process (with maximum and mean melt depths), LM

laser remelting process, and their thickness was not uniform. The coatings differed from each other depending on the remelting process parameters. The coating remelted with 2500 W power and 0.5 m/min speed was the most diverse in terms of thickness (especially the last very deep remelt was noticeable). Typically, the last remelt is the deepest due to the accumulation of heat in the material being remelted. The coatings that were remelted with the lowest laser power (1900 W) showed the greatest remelting uniformity. It was observed that the thickness of coating was also dependent on the applied remelting speed. The thickness of coating remelted with 0.5 m/min was less than coating remelted with 0.3 m/min. The higher the power of the melting beam, the more uneven the thickness of the coating. The widths of the remelted coatings had very similar values, which are marked in Fig. 2.

Figs. 3 and 4 presents a set of microphotographs of the coatings obtained at different magnifications by light microscopy and scanning electron microscopy, respectively. The remelted coatings, in all cases, were characterized by a cellular-dendritic structure. At the remelt line, the arrangement of dendrites along the direction of heat transfer can be noticed. In the case of coatings remelted with higher speed (0.5 m/min), the obtained dendritic structure is finer than that for the remelted coating with a speed of 0.3 m/min.

During microstructural observation of the coatings that were remelted with higher laser speed (0.5 m/min), discontinuities in the form of cracks were noticed (Fig. 5). Whereas the coating remelted with 0.3 m/min was free from cracks. The observed cracks are characteristic due to their location (initiating at the level of the fusion line and propagating from the substrate into the depth of the remelted coating). The occurrence of cracks is related to the stresses that occur during the laser remelting process and the rate of heat transfer during solidification. Moreover, it can be noticed that there is a correlation between the power of the applied laser and the existing cracks. The laser power influenced the crack lengths. In the case of the highest laser power (2500 W), the existing discontinuity has the greatest length.

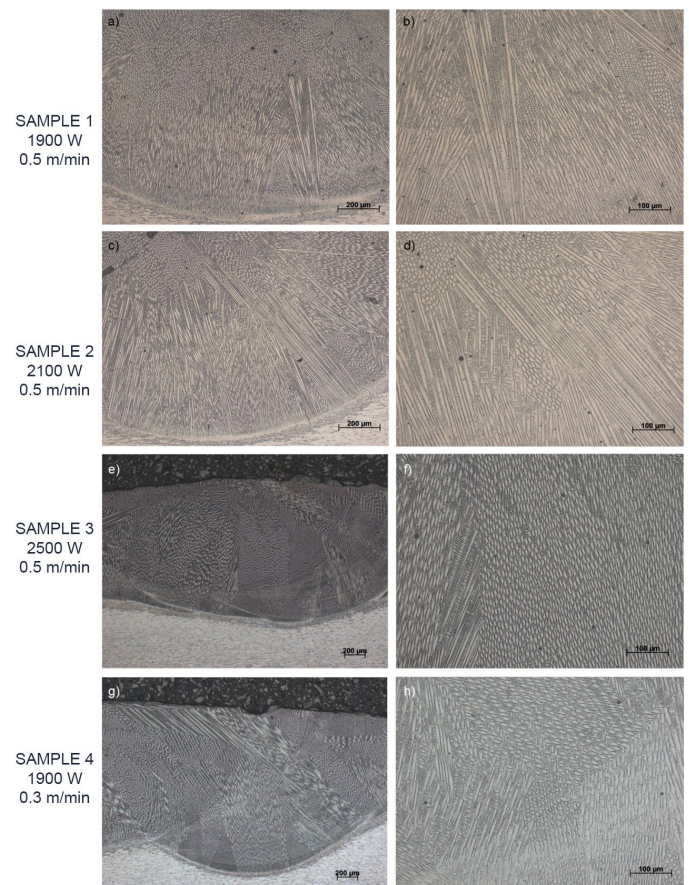


Fig. 3. Microstructure of the remelted coatings, LM

TABLE 3 presents the results of EDS analysis for the tested coatings. Analysis of the chemical composition indicated high iron content in the remelted coatings (above 40%). Iron comes from the substrate (316Ti steel). The coatings remelted with 0.5 m/min show lower iron content than the coating remelted with 0.3 m/min. Slower remelting causes greater fusion of the coating with the base material, hence the higher iron content (about 47%)

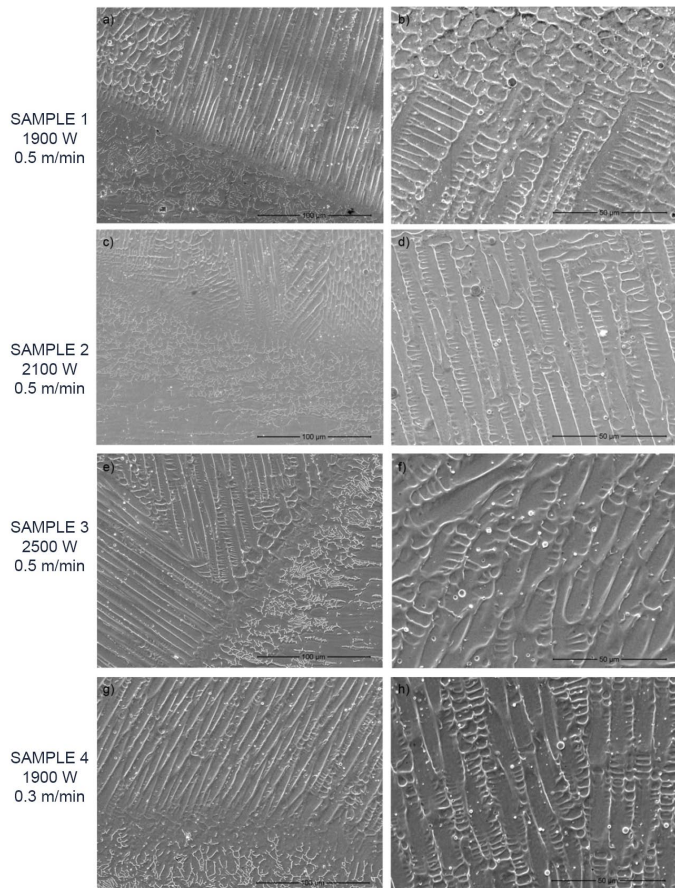


Fig. 4. Microstructure of the remelted coatings, SEM

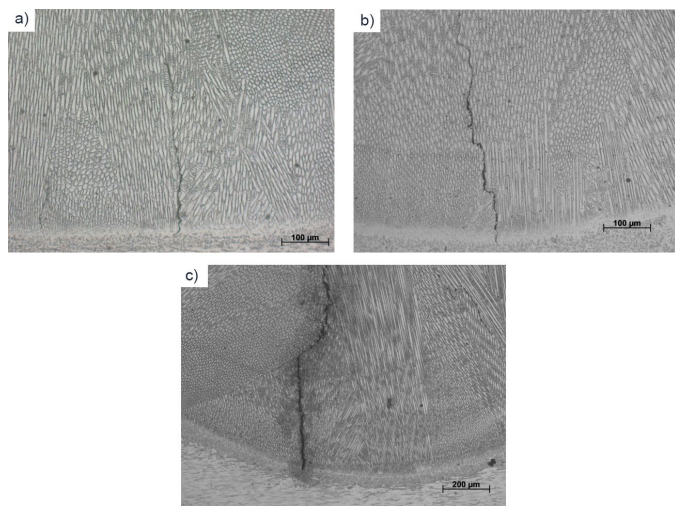


Fig. 5. Solidification cracking observed in the remelted coatings with 0.5 m/min speed and laser power a) 1900 W, b) 2100 W, c) 2500 W

and greater thickness (observed in Fig. 2). The average content of rhenium was 8% (for laser speed of 0.5 m/min) and 6% (for laser speed of 0.3 m/min).

Additionally, point EDS analysis was performed inside the dendrites and within the interdendritic spaces. Figs. 6 and 7 show an exemplary location of analysis points with exemplary spectra and quantitative analysis for dendrites and interdendritic spaces, respectively. Quantitative analysis was carried out for two values

of an accelerating voltage (5 kV and 15 kV). The accelerating voltage influenced the depth of analysis. When using a lower accelerating voltage, a higher content of chromium was observed in both the interdendritic spaces and dendrites.

TABLE 3

Average chemical composition of remelted coatings (wt.%) – EDS analysis

Element	1900 W 0.5 m/min	2100 W 0.5 m/min	2500 W 0.5 m/min	1900 W 0.3 m/min
Ni	35.7	33.2	34.8	29.8
Cr	16.6	16.9	16.3	17.1
Re	8.5	8.1	7.8	6.2
Fe	39.2	41.8	41.1	46.9

When comparing the results of the quantitative analysis, the areas of dendrites and interdendritic spaces differ in rhenium content. The dendrites were richer in rhenium in comparison to the interdendritic spaces. Microsegregation of other elements was not observed.

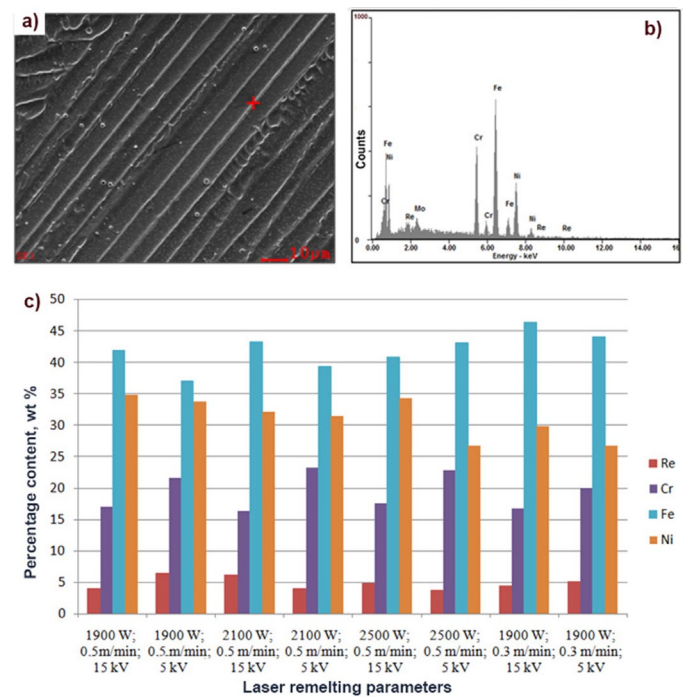


Fig. 6. EDS analysis in the dendrites a) exemplary analysed point b) exemplary spectrum c) content (in wt.%) of nickel, chromium, rhenium and iron depending on the remelting parameters and accelerating voltage

Plasma sprayed coatings were characterized by high heterogeneity of structure and chemical composition; therefore, their hardness was low and amounted to 75±9 HV0.3. The microhardness measurements were also performed for the remelted coatings in two paths (the first and the deepest remelts). The microhardness profiles are presented in Fig. 8. The coatings were characterized by inhomogeneous microhardness distribution, especially for the deepest remelt, what is related to heat accumulation in the material. In case of the deepest remelt, the

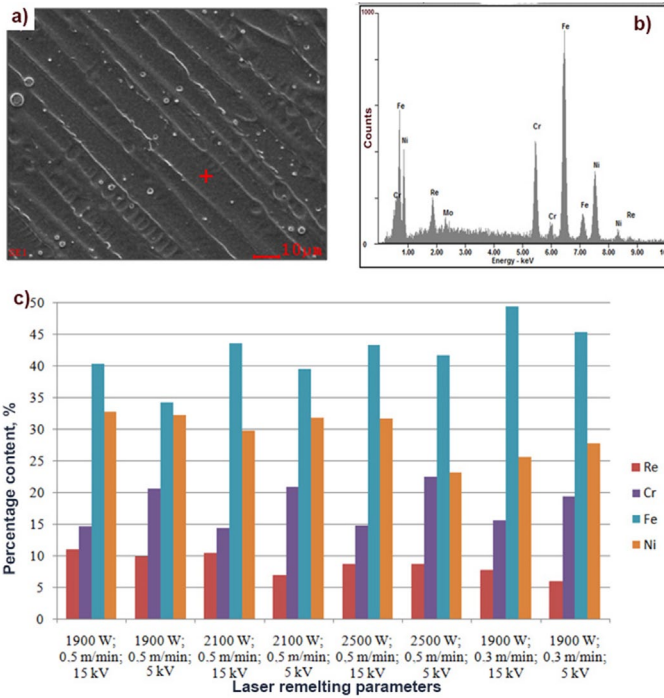


Fig. 7. EDS analysis in the interdendritic spaces a) exemplary analysed point b) exemplary spectrum c) content (in wt.%) of nickel, chromium, rhenium and iron depending on the remelting parameters and accelerating voltage

most consistent profile was noticeable for the coating remelted with a power of 2100 W and a speed of 0.5 m/min. The lowest values of microhardness were obtained for the coating remelted with a lower speed (0.3 m/min). The largest fluctuations in microhardness were observed in the case of the coatings remelted with power 1900 W and speed 0.5 m/min, but the coatings were characterized by the highest microhardness (205 HV0.3) at the surface.

Microhardness distribution in the first remelt for all tested coatings (Fig. 8b) are more regular compared to the first remelt. For the coatings remelted with 1900 W and 2500 W with 0.5 m/min, the hardness reaches values above 200 HV0.3. The lowest hardness of the remelted coating (approx. 160 HV0.3) and the most homogenous occurred in the coating remelted with speed of 0.3 m/min. All tested coatings were characterized by

hardness similar to that of the substrate material. This is related to the overly deep remelting of the base material, which was revealed by EDS results (about 40% of iron in the coatings). The remelting parameters were chosen to remelt the coatings; however, it was not possible to inhibit iron coming from the substrate. This is related to the too high melting point of rhenium. The high iron content in the coatings results in a hardness similar to that of the substrate.

4. Conclusions

In the present work, the microstructure, chemical composition and microhardness of plasma-sprayed and laser remelted Ni-Cr-Re coatings depending on the remelting parameters were investigated. The obtained results led to the formulation of following conclusions:

1. The laser remelting process demonstrates the ability to improve the quality of plasma sprayed Ni-Cr-Re coatings. Reduction of the porosity and an increase in the chemical composition homogeneity are evident.
2. The thickness of the remelted coatings was irregular. Reducing the laser power also results in a more uniform coating thickness. Additionally, stress cracks were observed in all coatings remelted at the higher laser speed (0.5 m/min).
3. The remelted coatings were characterized by a dendritic microstructure. Microsegregation of rhenium to dendrites was observed.
4. The remelted coatings have an iron content of over 40%, which is the result of too deep remelting with the substrate material. The iron content in the remelted coatings increases with the decrease in laser speed, but the rhenium content decreases.
5. The high iron content in the coatings results in a hardness similar to that of the substrate.

Acknowledgements

This work has been performed with funding from National Science Centre in Poland within the frame of the research grant UMO-2018/29/B/ST8/01206

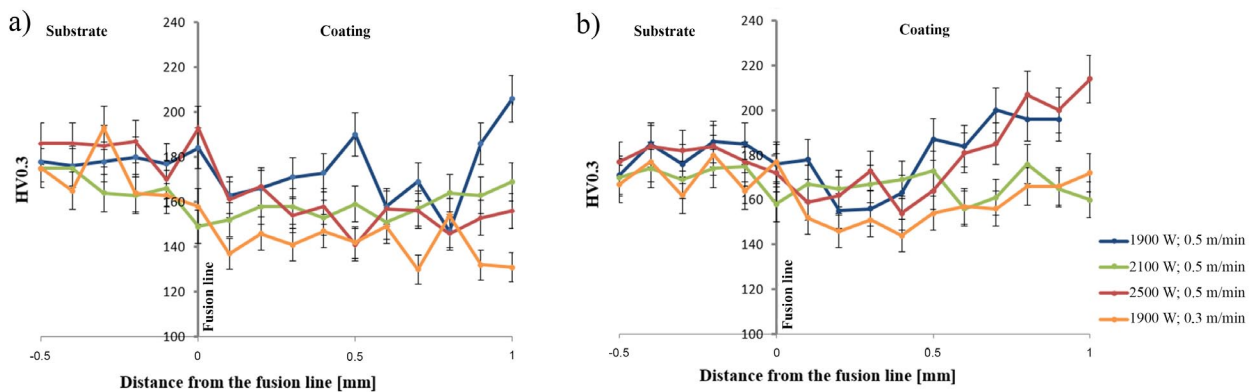


Fig. 8. Microhardness (HV0.3) distribution in the remelted coatings a) the deepest remelt, b) the first remelt

entitled: "Multi scale analysis of microstructural changes in wear resistant coatings produced by plasma spraying followed by remelting with an application of concentrated energy sources in view of the improvement of their mechanical properties".

REFERENCES

- [1] K.G. Bundinski, Prentice-Hall, Surface Engineering for Wear Resistance, New Jersey 1988.
- [2] M.K. Hobbs, H. Reiter, Residual stresses in ZrO₂-8%Y₂O₃ plasma sprayed thermal barrier coatings. Thermal Spray: Advances in Coatings Technology, ASM International 1989.
- [3] A. Klimpel, Wydawnictwo Naukowo-Techniczne, Napawanie i natryskiwanie cieplne, Warszawa 2000.
- [4] S. Özel, E. Vural, The microstructure and hardness properties of plasma-sprayed Cr₂O₃/Al₂O₃ coatings. J. Optoelectron. Adv. Mater. **18**, 1052-1056 (2016).
- [5] F.J. Hermanek, Wear-Resistant Quasicrystalline Coating. U.S. Patent 6,254,699 (2001).
- [6] M.F.O. Schiefler Filho, A.J.A. Buschinelli, F. Gärtner, A. Kirsten, J. Voyer, H. Kreye, Influence of process parameters on the quality of thermally sprayed X46Cr13 stainless steel coatings. J. Braz. Soc. Mech. Sci. Eng. **26**, 98-106 (2004)
- [7] S. Hazra, J. Das et al., Synthesis of mullite-based coatings from alumina and zircon powder mixtures by plasma spraying and laser remelting. Materials Chemistry and Physics **154**, 22-29 (2015).
- [8] C. Zhu, P. Li et al., An investigation on the microstructure and oxidation behavior of laser remelted air plasma sprayed thermal barrier coatings. Surface & Coatings Technology **206**, 3739-3746 (2012).
- [9] A. Grabowski, B. Formanek et al., Laser remelting of Al-Fe-TiO powder composite on aluminium matrix. Journal of Achievements in Materials and Manufacturing Engineering **33** (1) 78-85 (2009).
- [10] B. Das, A.K. Nath et al., Online monitoring of laser remelting of plasma sprayed coatings to study the effect of cooling rate on residual stress and mechanical properties. Ceramics International **44**, 7524-7534 (2018).
- [11] A. Klimpel, L. Dobrzyński, et al., The study of the technology of laser and plasma surfacing of engine valves face made of X40Cr-SiMo10-2 steel using cobalt based powders. Journal of Materials Processing Technology **175** (1-3), 251-256 (2006).
- [12] K. Majchrowicz, Z. Pakieła, J. Kamiński, et al., The Effect of Rhenium Addition on Microstructure and Corrosion Resistance of Inconel 718 Processed by Selective Laser Melting. Metall. Mater. Trans. A. **49**, 6479-6489 (2018).
- [13] Noh Sanghoon, Kang Suk Hoon, Kim Tae, Effect of Rhenium Addition on Microstructures and Mechanical Properties of Oxide Dispersion Strengthened Ferritic Steels. Archives of Metallurgy and Materials **65**, 1261-1264 (2020).
- [14] T. Kurzynowski, I. Smolina, et al., Wear and corrosion behaviour of Inconel 718 laser surface alloyed with rhenium. Materials & Design **132**, 349-359 (2017).
- [15] A. Wrona, M. Lis, et al., Ni-Cr powders modified with rhenium as a novel coating material – physical properties, microstructure, and behavior in plasma plume. Materials **15**, 11, 1-16 (2022).